Numerical investigation of G-V measurements of metal - A nitride GaAs junction

A. Ziane[a], A. Rabehi[b,c], A. Rouabhia[a], M. Amrani[b], A. Douara[d],
R. Dabou[a], A. Necaibia[a], M. Mostefaoui[e], and N. Sahouane[a]

[a]*Unité de Recherche en Energies Renouvelables en Milieu Saharien, URERMS,
Centre de Développement des Energies Renouvelables, CDER, 01000, Adrar, Algeria.*
[b]*Laboratoire de Micro-électronique Appliqué, Université Djillali Liabes de Sidi Bel Abbés,
BP 89, 22000, Sidi Bel Abbés, Algeria.*
[c]*Laboratory of Telecommunications and Smart Systems, Faculty of Science and Technology,
University of Djelfa, PO Box 3117, Djelfa, Algeria.*
[d]*Institute of Science and Technology, Tissemsilt University Center,
38000 Tissemsilt, Algeria.*
[e]*École Supérieure d'Agriculture Saharienne d'Adrar, Adrar, Algeria.*

Received 12 February 2024; accepted 21 June 2024

In this study, a Schottky diode consisting of Au/GaN/GaAs was fabricated using a radiofrequency nitrogen plasma source. The voltage-conductance characteristics (G/ω-V) of this diode structure were investigated at room temperature. To interpret the changes in the electrical properties of the nitrided GaAs-based Schottky structure, we developed a simulation program. This program employs a numerical model to calculate the G-V characteristics, allowing us to validate the experimental measurements conducted on the Schottky diodes. The geometric model used in our simulation considers not only the GaN layer formed between the metal and GaAs substrate but also the density and distribution of trapped states within the band gap. The program utilizes the numerical resolution of the Poisson and continuity equations to calculate the electrostatic potential and the concentrations of both n and p mobile carriers. These parameters are then used to determine the electric charge, current, capacitance, and conductance. The simulation results were subsequently compared to the experimental measurements to ensure their accuracy.

Keywords: MIS structure; G-V; trap states; surface nitridation.

DOI: https://doi.org/10.31349/RevMexFis.70.061604

1. Introduction

Due to its remarkable physical properties (direct band gap, high electron mobility ...) [1], Gallium Arsenide is used in the production of optoelectronics components [2,3] and hyperfrequency devices [4]. However, the major disadvantage of the GaAs substrate is its strong surface recombination [5] which increases the device noise and the leakage current [6]. Furthermore, the performance of electronic components is primarily determined by the quality of the material's surface [7]. To improve GaAs surface characteristics, various techniques have been employed. Among these techniques, we adopted the restructuring of the surface by exposing a GaAs substrate to active nitrogen plasma created by a low-power GDS source, leading to the creation of quality GaN layers. The GaN offers thermal and chemical stability [8] unlike group III oxides [9] and can significantly decrease the surface recombination velocity [10]. Extensive efforts have been dedicated to the exploration of nitride GaAs Schottky diodes for several years. In the study by Benamara [10], x-ray photoelectron spectroscopy (XPS) and photoluminescence surface state spectroscopy (PLS3) were employed to ascertain the properties of GaN/GaAs (100). Additionally, the effect of temperature on the forward and reverse bias characteristics of GaN -based Schottky diodes has been investigated by Sharma [12]. Ebeoğlu [8] focused on investigating the current-voltage characteristics of the Au/GaN/GaAs structure achieved through the chemical anodic nitridation method. Kacha [13] examined the effects of GaN layers and annealing on the electrical properties of Schottky diodes based on nitrided GaAs. Furthermore, the electrical and photoelectrical properties of GaN/Au/GaAs were studied by Rabehi [14]. In the same context Helal [15] conducted a comparative study of ionic bombardment and heat treatment on the electrical behavior of Au/GaN/n-GaAs Schottky diodes. In this article, we fabricated the Au/GaN/GaAs structure through the nitridation process of the GaAs substrate. The substrate was exposed to a nitrogen flow generated by a discharge source with high voltage under ultra-high vacuum conditions [16]. In our previous studies, we conducted frequency-related measurements of the Au/GaN/GaAs structure including the modeling and simulation of the C-V measurements of an Au/GaN/GaAs structure [17] and the evaluation of low and high-frequency capacitance of this structure [18]. In this work, our focus lies in studying and modeling the interface properties of the Au/GaN/GaAs diode using experimental G-V characteristics measured at various frequencies. Our goal is to establish a reliable simulation model for the $G-V$ characteristics with a continuous energy distribution of interface states [19].

2. Material and method

2.1. Experimental elaboration

In this study, a unique radio frequency discharge nitrogen plasma source, extensively described in Matolín's work [20], was employed for the nitridation process. The nitridation process involved the production of continuous nitrogen plasma at a power level of 5W, resulting in the creation of a majority of N atomic species. The specific parameters used for this process included a nitrogen pressure of 1.33×10^{-5} Kpa, an ion energy of 2.5 keV, and a sample current of 1 μA/cm^2. For this work, an n-type GaAs (100) substrate with a concentration of $Nd = 4.9 \times 10^{15}$ cm^{-3} and a thickness of $400 \pm 20\ \mu$ was utilized. The cleaning procedure for the samples followed a common practice [21], involving sequential chemical cleaning in H_2SO_4, deionized water, and cold and hot methanol, with the assistance of ultrasound. The samples were then dried using $N2$ and subjected to $Ar+$ ion bombardment within an ultra-high vacuum (UHV) chamber. The ion bombardment process had an ion energy of 1 keV, a sample current of 5 μA/cm^2, and lasted for 1 hour. Before the nitridation process, the GaAs (100) substrate was heated to 500°C for a duration of 1 hour. Subsequently, the samples were exposed to a nitrogen flow for a chosen duration of 5 minutes.

The experimental procedures were conducted within a custom-built ultra-high vacuum (UHV) chamber, which was equipped with an X-ray photoelectron spectroscopy (XPS) system consisting of a dual-anode Al-Mg X-ray source and a hemispherical electron energy analyzer. This setup enabled us to determine the chemical composition and crystal structure of the samples under investigation. For the XPS experiments, we utilized a Mg K-alpha source with an energy of 1253.6 eV, and the incident angle was set at 55° for normal detection. The pass energy of the analyzer was maintained at 20 eV. Details of the preparation parameters specific to our sample can be found in Table I. The electrical testing of the structure involved the use of an Au contact, where the contact area and thickness were specified as $S = 4.41 \times 10^{-3}$ cm^2 and $d = 100$ nm, respectively. In order to enhance the quality of the Ohmic contact, a layer of tin (Sn) was deposited on the back face using NH4Cl at a temperature of 350°C for a duration of 5 minutes. This deposition process aimed to prevent the formation of oxides and other impurities on the surface of GaAs, which facilitates improved diffusion of Sn into GaAs.

TABLE I. Preparation parameters of the sample.

Parameter	Value
GaAs concentration	$Nd = 4.9 \times 10^{15}$ cm^{-3}
Nitridation conditions	500°C 5W, 5 min
Annealing	620°C at 60 min
GaN thickness	0.7 nm
Metal contact	Au
Ohmic contact	Sn

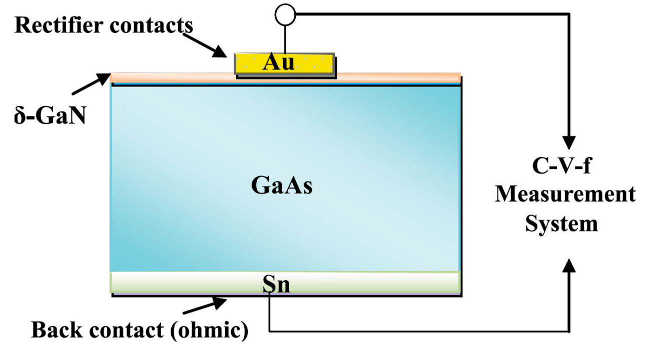

FIGURE 1. Schematic of $Au/GaN/GaAs$ diode.

To conduct the capacitance-voltage $(C - V)$ measurements, various frequencies were employed, namely 1 MHz, 500 KHz, 100 KHz, 10 KHz, and 1 KHz. The measurements were performed at room temperature using a Keithley test system with a 590 $C - V$ analyzer.

2.2. G-V-f measurements

Schottky diode conductance-voltage measurements are an experimental technique employed to examine the electrical characteristics of a Schottky diode in relation to the applied voltage. This technique involves measuring the conductance or resistance of the diode at various voltage levels. Plotting the conductance against the voltage allows for the extraction of important diode parameters, including barrier height, series resistance, and interface properties. These measurements offer valuable insights into the behavior and performance of Schottky diodes across different applications. Figure 2 presents the conductance of the Au/GaN/GaAs structure as a function of the applied voltage at various frequencies ranging from 1 kHz to 1 MHz, all measured at room temperature (300 K). The applied voltage spanned from -2 V to $+2$ V. The curves of $G/\omega - V$ demonstrate that the conductance G/ω is affected by both the bias voltage and the frequency.

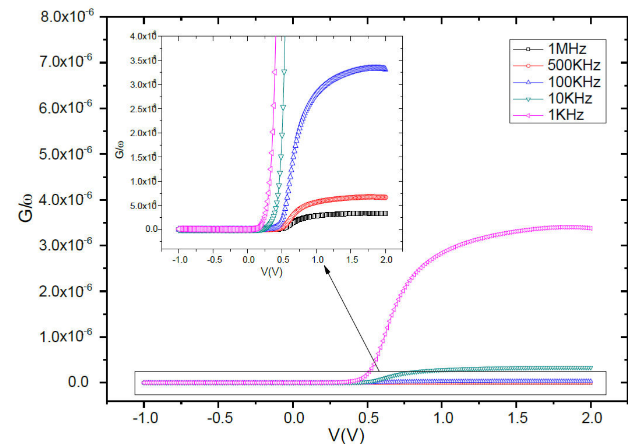

FIGURE 2. Schematic of Variation de $G/\omega - V$ of Au/GaN/GaAs for various frequencies diode.

2.3. Structure modeling

Due to the fact that the Au/GaN/GaAs heterostructure can be modeled by basic semiconductor equations, Poisson and continuity equations are as follows:

$$\frac{\partial^2\varphi}{\partial^2 x} = \frac{q}{\varepsilon}(-p + n - p_T + n_T - N_D^+ + N_A^-), \quad (1)$$

$$\frac{1}{q}\frac{\partial j_n}{\partial x} = U_n, \quad (2)$$

$$\frac{1}{q}\frac{\partial j_p}{\partial x} = -U_p. \quad (3)$$

Here, φ is the electrostatic potential, ε the dielectric constant, n and p are the density of electron and holes, its equations are as follow:

$$n = N_c \exp\left[\frac{-(E_c - E_{Fn}))}{kT}\right], \quad (4)$$

$$N_c = 2\left(\frac{2m_c^* kT}{h^2}\right)^{\frac{3}{2}}, \quad (5)$$

$$p = N_v \exp\left[\frac{-(E_{Fp} - E_v)}{kT}\right], \quad (6)$$

$$N_v = 2\left(\frac{2m_v^* kT}{h^2}\right)^{\frac{3}{2}}, \quad (7)$$

N_D^+, N_A^- are the doping concentrations with the assumption of totally ionized impurities, n_t and p_t are the concentrations trapped carriers of electrons in the acceptor states and holes in the donor states which are [24]:

$$n_t = \int_{E_V}^{E_C} y_D(E_t) f_{ct}(E_t) dE_t, \quad (8)$$

$$p_t = \int_{E_V}^{E_C} y_A(E_t) f_{vt}(E_t) dE_t. \quad (9)$$

In this context, y_A represents the density of acceptor states per unit volume and energy, while y_D represents the density of donor states per unit volume and energy. E_t denotes the energy level of the defect state located within the band gap. Under thermal equilibrium conditions, the functions $f_{ct}(E)$ and $f_{vt}(E)$ represent the occupation functions of the acceptor and donor traps, respectively, as dictated by the Schockley-Hall-Read kinetics [23]:

$$f_{ct}(E) = \frac{C_n^{ct} p + C_p^{vt} n_1(E))}{C_p^{vt}(p + p1(E)) + C_n^{ct}(n + n1(E))}, \quad (10)$$

$$f_{vt}(E) = 1 - f_{ct}(E) = \frac{C_n^{ct} n + C_p^{vt} p_1(E))}{C_p^{vt}(p + p1(E)) + C_n^{ct}(n + n1(E))}, \quad (11)$$

where C_n^{ct}, C_p^{ct}, C_n^{vt}, C_p^{vt} are respectively the electron capture sections and the holes by the valence band and conduction edges. For the generation-recombination rate U, one finds

$$U = U_n = U_p = \int_{E_v}^{E_c}\left[y_A(E) \times \frac{\alpha_{nA}\alpha_{pA} np - e_{nA}e_{pA}}{\alpha_{nA} n + e_{nA} + \alpha_{pA} p + e_{pA}} + y_D(E)\frac{\alpha_{nD}\alpha_{pD} np - e_{nD}e_{pD}}{\alpha_{nD} n + e_{nD} + \alpha_{pD} p + e_{pD}}\right], \quad (12)$$

where e_{nA}, e_{pA}, e_{nD}, e_{pD}, are the emission rates and α_{nA}, α_{pA}, α_{nD}, α_{pD} are the capture constants, respectively. There are various models of the continuous distribution of traps states form the exponential model Gaussian model and uniform model [24].

The interface state density of $GaAs$ structure is observed to be a U-shaped localized state continuum extending over the entire bandgap by Hasegawa [25], meaning that the interface state density increases exponentially from the midgap to the band edge.

$$N_{VT}(E) = N_{VT0} \exp\left(\frac{E_V - E}{kT_v}\right), \quad (13)$$

$$N_{CT}(E) = N_{CT0} \exp\left(\frac{E - E_C}{kT_c}\right). \quad (14)$$

Here, kT_c and kT_v are the characteristic levels respectively of the acceptor and donor states and N_{CT0}, N_{VT0} are the densities per unit of energy respectively at the edge of the conduction and valence band. Several studies suggested a Gaussian distribution for nitride MIS structures [26-29], the Gaussian distribution of states for donor and acceptor trapping states are:

$$N_{dbaT}(E) = N_{GA} \exp\left(-\left[\frac{E - E_{GA}}{W_{GA}}\right]^2\right), \quad (15)$$

$$N_{dbd}(E) = N_{GD} \exp\left(-\left[\frac{E - E_{GD}}{W_{GD}}\right]^2\right). \quad (16)$$

In the context of our study, (N_{GA}, N_{GD}) represents the maximum density of interface states, while (W_{GA}, W_{GD}) corresponds to the standard deviation of the Gaussian distribution. Additionally, (E_{GD}, E_{GA}) denotes the peak position of the interface state distribution.

To achieve a more comprehensive representation, our investigation incorporates both Gaussian and exponential distributions. The energetic distribution of trap states is obtained through the superposition of two exponential distributions and two Gaussian distributions for acceptor and donor states,

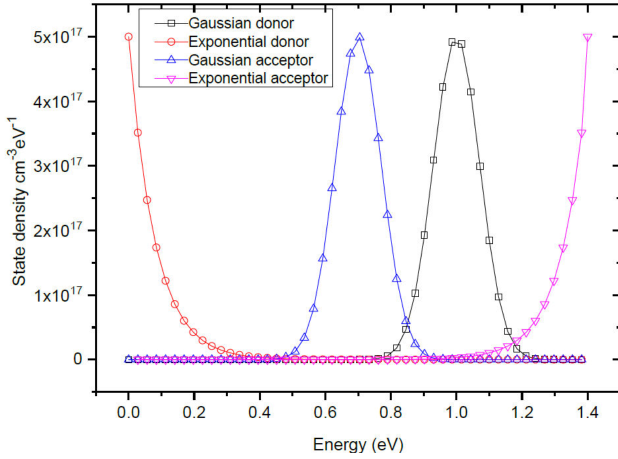

FIGURE 3. Gaussian and Exponential distribution profiles of continuous state density in bandgap.

as depicted in Fig. 3. The total interface state distribution for acceptor and donor states is as follows:

$$y_A(E) = N_{VT0} \exp\left(\frac{E_V - E}{kT_v}\right) + N_{GA} \exp\left(-\left[\frac{E - E_{GA}}{W_{GA}}\right]^2\right), \quad (17)$$

$$y_D(E) = N_{CT0} \exp\left(\frac{E - E_C}{kT_c}\right) + N_{GA} \exp\left(-\left[\frac{E - E_{GA}}{W_{GA}}\right]^2\right). \quad (18)$$

The differential conductance of the structure has been calculated as follow:

$$G = \frac{\Delta i}{\Delta i}, \quad (19)$$

where Δi is the difference in the electrical current in the structure for two very close external voltages with difference Δi [30].

2.4. Computational solution

Computational solutions have numerous advantages over analytical methods. They offer flexibility to handle complex equations and models without analytical solutions, making them suitable for nonlinear and multidimensional problems. They are efficient, processing large datasets quickly and saving time compared to manual approaches. Computational solutions excel in accuracy, especially for intricate systems with multiple variables, providing realistic outcomes through numerical approximations. They can handle complex geometries, boundary conditions, and simulate real-world scenarios accurately. Overall, computational solutions revolutionize scientific and engineering fields by providing flexibility, efficiency, accuracy, and the capability to handle complex systems and scenarios. For those reasons, we used a computational solution to solve the equation over an analytical one. Solving the system of equations in this study poses a challenge due to the numerous unknown variables involved. To simplify the system, we reduce it to three unknowns: the electrostatic potential ϕ , and the concentrations of n and p carriers. However, the presence of exponential terms in the expressions for n and p introduces strong non-linearity into the resulting equations. To address the nonlinearity introduced by the exponential terms in the expressions for n and p, we discretize the partial differential equations using the finite differences method. The grid is constructed with non-equally spaced points, ensuring sharp discretization at the junction (GaN/GaAs) for accurate calculations [31]. This approach involves replacing the differential equation with a difference equation after discretizing the study domain. We employ the Gummel algorithm [32] to solve the system. This algorithm solves the three equations successively, with each equation based on estimated solutions for the other two unknowns. The corrected value of each unknown is then updated in the subsequent equation. This iterative process continues until convergence is achieved for all three equations.

3. G-V Characteristic simulation

3.1. Work function effect

The work function is the minimum energy needed to extract an electron from the surface of a material and transport it to a point immediately outside the material. Measured in electron volts (eV), the work function varies for different materials. It signifies the energy barrier that electrons must overcome to escape the material, playing a significant role in comprehending electronic phenomena like electron emission, the photoelectric effect, and the formation of Schottky barriers in electronic devices. The work function relies on factors such as the material's electronic structure, surface properties, and temperature. In electronics, the output work is an important quantity for the design of metal-semiconductor junctions of Schottky diodes. In recent years, many studies have estimated gold work function values between 4.8 and 5.47 eV [33,34].

We studied the effect of work function variations on the conductance-voltage $(G - V)$ characteristics of a Schottky Au/GaN/GaAs structure using the developed simulation program. Figure 4 illustrates the impact of work function variation on the G-V characteristic of the Au/GaN/GaAs diode. By fixing the other parameters- the doping concentration $Nd = 5.1014$ cm^{-3} and the state distribution profile of the interface with tail state values of the density bands ($NCT0 =$ 1010 cm-2 eV^{-1} $NVT0 = 1010$ cm^{-2}eV^{-1}) and Gaussian peak parameters ($NGD = NGA = 1010$ cm^{-2}eV^{-1}). We observed that the value of the gold work function significantly influences the $G - V$ characteristics of the structure, particularly the threshold voltage. An increase in the gold work function shifts the curve upwards and increases the threshold voltage, while the maximum value of conductance remains unchanged.

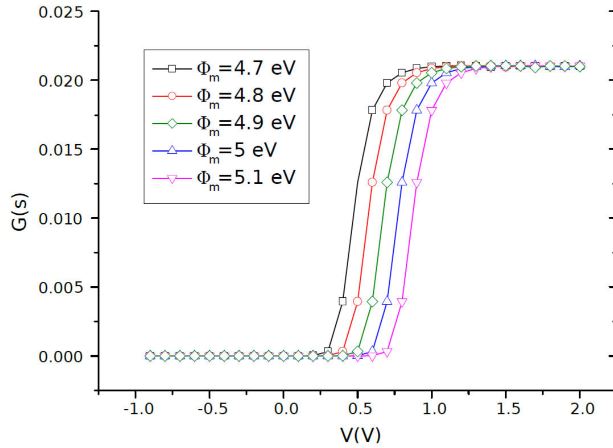

FIGURE 4. Simulated $G - V$ characteristics for several ϕ_m values of gold.

We observed that the value of the gold work function significantly influences the $G - V$ characteristics of the structure, particularly the threshold voltage. An increase in the gold work function shifts the curve upwards and increases the threshold voltage, while the maximum value of conductance remains unchanged. These findings highlight the importance of the gold work function in tuning the electrical behavior of the Au/GaN/GaAs Schottky diode. Adjusting the work function allows for precise control over the threshold voltage, which can be critical for optimizing the diode's performance in various applications. However, the constancy of the maximum conductance value suggests that while the threshold voltage can be modulated, the overall conductive capacity of the diode is maintained.

3.2. Doping effect

The effect of doping concentration was examined using our low frequency conductance simulation program by varying the uniform doping concentration from 2×10^{13} to 10^{15} cm^{-3} as shown in Fig. 5. The Examination of Fig. 5 indicates that the doping concentration has a direct relationship with the conductance of the structure in the forward bias regime, in contrast to the reverse regime, the effect of the doping concentration is negligible.

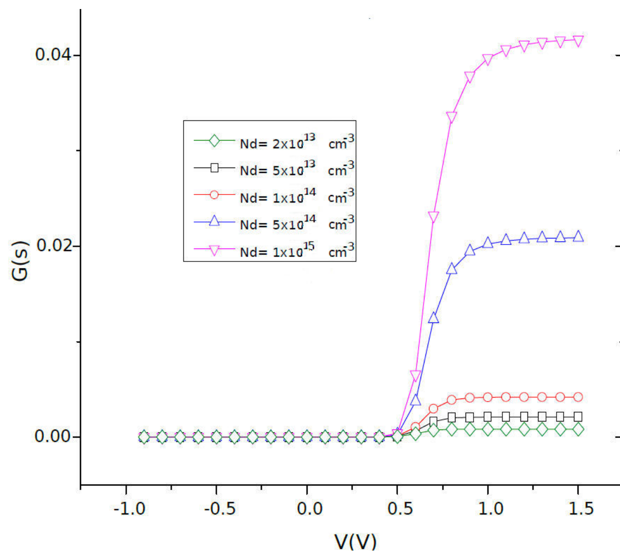

FIGURE 5. Simulated G-V characteristics for multiple doping concentrations.

The maximum value of the conductance increases by 8×10^{-4} s for a doping concentration equal to 2×1013 cm^{-3} and 4×10^{-2} s for a doping concertation of the order 1×1015 cm^{-3}. When the doping concentration increases, the maximum value of the conductance of the diode also increases. This phenomenon can be explained by the fact that doping introduces additional charge carriers into the structure, which enhances conductivity and subsequently increases the current flow. As more charge carriers are available, the material becomes more conductive, allowing for greater current at a given voltage. In light of the simulation results, the effect of doping on the conductance-voltage $(G-V)$ characteristics in a Schottky diode can be further detailed. Higher doping concentration increases the number of charge carriers in the semiconductor material. This enhanced carrier density significantly improves the diode's conductivity. Consequently, with more available carriers, the diode can support a higher current flow for a given voltage, leading to an increase in the maximum conductance observed in the G-V characteristics. This relationship demonstrates how modifying the doping concentration can effectively tune the electrical performance of a Schottky diode. By carefully controlling the level of doping, it is possible to optimize the diode's conductance properties, thereby improving its overall functionality in various applications.

3.3. Experimental fitting

The comparison between the simulated quasi-static $G - V$ curve with experimental low-frequency measurements (1 kHz) is shown in Fig. 6. We adjusted the two curves with the following parameters: the work function of the gold, the doping concentration and thus the distribution of the states of the interface.

We can see in Fig. 6 that the low-frequency G-V experimental characteristics (1 KHz) and the simulated G-V characteristics have sufficient agreement. This adjustment was obtained for the interface distribution profile uw (gaussian and exponential) interface with values of the density band tails states ($NCT0 = 1010$ cm^{-2}eV^{-1}, $NVT0 = 1010$ cm^{-2}eV^{-1}) and Gaussian peak parameters ($NGD = NGA = 1010$ cm^{-2}eV^{-1}) and doping concentration of 1014 cm^{-3} and gold work function of 4.9 eV. The results obtained indicate that the doping concentration estimated by the simulation is lower than that provided by the supplier. This discrepancy can be attributed to the effect of annealing on the carrier concentration; several studies have shown that annealing at temperatures above 600°C can significantly reduce the carrier concentration [35,36]. Our program is based on a valid quasi-static model for low frequencies, which can

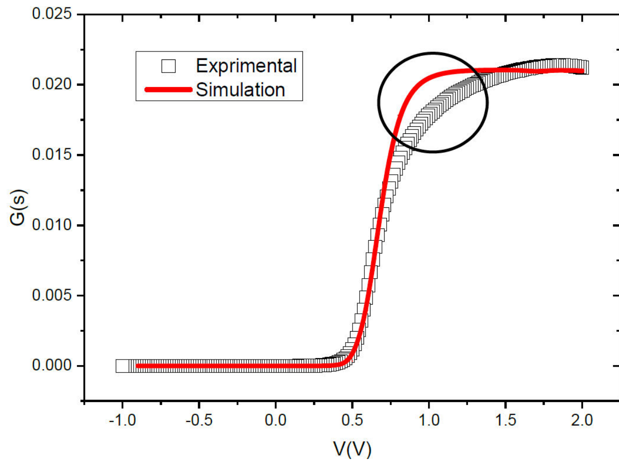

FIGURE 6. Experimental and simulated G-V characteristics at low frequency.

slightly disagree with experimental features including; the characteristic $G-V$.

4. Conclusions

This study investigated a Schottky diode based on Au/GaN/GaAs, fabricated using a radiofrequency nitrogen plasma source. The diode's voltage-conductance characteristics ($G/\omega - V$) were explored across frequencies from 1 kHz to 1 MHz, revealing significant frequency-dependent behavior due to interface states. A 1D simulation program was developed to analyze the electrical characteristics of the Au/GaN/GaAs diode. By studying various parameters, we found that doping concentration affects the diode's conductance, with higher doping levels increasing maximum conductance by introducing additional charge carriers. Furthermore, the gold work function was found to influence the diode's threshold voltage. An increase in the work function raised the threshold voltage while maintaining a constant maximum conductance. Future work will involve developing a 2D numerical simulation program to delve deeper into the electrical behavior of these structures. This will aid in optimizing GaAs-based structures through better control of their electrical properties.

1. J. Yoon, GaAs photovoltaics and optoelectronics using releasable multilayer epitaxial assemblies, Nature 2010 465:7296 **465** (2010) 329, https://doi.org/10.1038/nature09054.

2. O. Wada, Optoelectronic integration based on GaAs material, Optical and Quantum Electronics **20** (1988) 441, https://doi.org/10.1007/BF00635747.

3. C. J. S. Mokkapati, S. Mokkapati, and C. Jagadish, III-V compound SC for optoelectronic devices, Materials Today **12** (2009) 22, https://doi.org/10.1016/S1369-7021(09)70110-5.

4. F. Schwierz and J. J. Liou, RF transistors: Recent developments and roadmap toward terahertz applications, Solid-State Electronics **51** (2007) 1079, https://doi.org/10.1016/j.sse.2007.05.020.

5. R. J. Nelson, et al., Reduction of GaAs surface recombination velocity by chemical treatment, Applied Physics Letters **36** (1980) 76, https://doi.org/10.1063/1.91280.

6. M. Ambrico, et al., A study of remote plasma nitrided nGaAs/Au Schottky barrier, Solid-State Electronics **49** (2005) 413, https://doi.org/10.1016/j.sse.2004.11.007.

7. Interface states density distribution in Au/n-GaAs Schottky diodes on n-Ge and n-GaAs substrates, Materials Science and Engineering B: Solid-State Materials for Advanced Technology **87** (2001) 141, https://doi.org/10.1016/S0921-5107(01)00713-9.

8. M. A. Ebeoglu, Current-voltage characteristics of Au/GaN/GaAs structure, Physica B: Condensed Matter **403** (2008) 61, https://doi.org/10.1016/j.physb.2007.08.008.

9. K. W. Vogt and P. A. Kohl, Gallium arsenide passivation through nitridation with hydrazine, *Journal of Applied Physics* **74** (1993) 6448, https://doi.org/10.1063/1.355130.

10. S. Anantathanasarn and H. Hasegawa, Surface Passivation of GaAs Using an Ultrathin Cubic GaN Interface Control Layer, *Journal of Vacuum Science Technology B: Microelectronics and Nanometer Structures* **19** (2001) 1589, https://doi.org/10.1116/1.1388605.

11. Z. Benamara *et al.*, XPS, electric and photoluminescencebased analysis of the GaAs (1 0 0) nitridation, *Applied Surface Science* **252** (2006) 7890, https://doi.org/10.1016/j.apsusc.2005.09.056.

12. E. Sharma *et al.*, Effect of temperature on forward and reverse bias characteristics of GaN based Schottky diode, *Materials Today: Proceedings* **79** (2023) 324, https://doi.org/10.1016/j.matpr.2022.12.025.

13. A. Kacha, *et al.*, Effects of the GaN layers and the annealing on the electrical properties in the Schottky diodes based on nitrated GaAs, *Superlattices and Microstructures* **83** (2015) 827, https://doi.org/10.1016/j.spmi.2015.04.017.

14. A. Rabehi, *et al.*, Simulation and Experimental Studies of Illumination Effects on the Current Transport of Nitridated GaAs Schottky Diode, *Semiconductors* **52** (2018) 1998, https://doi.org/10.1134/S106378261816025X.

15. H. Helal, *et al.*, Comparative study of ionic bombardment and heat treatment on the electrical behavior of Au/GaN/n-GaAs Schottky diodes, *Superlattices and Microstructures* **135** (2019), https://doi.org/10.1016/j.spmi.2019.106276.

16. N. Zougagh, *et al.*, The dc Electrical Characterization of Hg/-GaN/n-GaAs Devices, with Different Thicknesses of the GaN Thin Layers, *Sensor Letters* **9** (2011) 2211, https://doi.org/10.1166/sl.2011.1817.

17. A. Ziane, *et al.*, Modeling and Simulation of Capacitance-Voltage Characteristics of a Nitride GaAs Schottky Diode, *Journal of Electronic Materials* (2018) 1, https://doi.org/10.1007/s11664-018-6408-1.

18. A. Ziane, *et al.*, Low- and High-Frequency C-V Characteristics of Au/n-GaN/n-GaAs, *International Journal of Nanoscience* **18** (2019) 1850039, https://doi.org/10.1142/S0219581X18500394.

19. M. Sakhaf and M. Schmeits, Capacitance and conductance of semiconductor heterojunctions with continuous energy distribution of interface states, *Journal of Applied Physics* **80** (1996) 6839, https://doi.org/10.1063/1.363750.

20. V. Matolın, *et al.*, Experimental system for GaN thin films growth and in situ characterisation by electron spectroscopic methods, *Vacuum* **76** (2004) 471, https://doi.org/10.1016/j.vacuum.2003.12.163.

21. L. L. Smith, *et al.*, Cleaning of GaN surfaces, *Journal of Electronic Materials* **25** (1996) 805, https://doi.org/10.1007/BF02666640.

22. M. Schmeits, Small-signal analysis of semiconductor heterojunctions with interacting interface states, *Semiconductor Science and Technology* **12** (1997) 1217, https://doi.org/10.1088/0268-1242/12/10/007.

23. D. K. Schroder, Semiconductor Material and Device Characterization (Wiley, 2005), https://doi.org/10.1002/0471749095.

24. N. Inoue, et al., Analysis of Interface States in LaSi x O y Metal-Insulator-Semiconductor Structures, *Japanese Journal of Applied Physics* **46** (2007) 6480, https://doi.org/10.1143/JJAP.46.6480.

25. H. Hasegawa and T. Sawada, Electrical modeling of compound semiconductor interface for FET device assessment, *Electron Devices, IEEE Transactions on* **27** (1980) 1055, https://doi.org/10.1109/T-ED.1980.19986.

26. B. Bakeroot, *et al.*, On the origin of the two-dimensional electron gas at AlGaN / GaN heterojunctions and its influence on recessed-gate metal-insulator-semiconductor high electron mobility transistors, *Journal of Applied Physics* **116** (2014) 134506, https://doi.org/10.1063/1.4896900.

27. M. Miczek, et al., Effects of interface states and temperature on the C-V behavior of metal/insulator/AlGaN/GaN heterostructure capacitors, *Journal of Applied Physics* **103** (2008) 104510, https://doi.org/10.1063/1.2924334.

28. T. Hashizume and H. Hasegawa, Effects of nitrogen deficiency on electronic properties of AlGaN surfaces subjected to thermal and plasma processes, *Applied Surface Science* **234** (2004) 387, https://doi.org/10.1016/j.apsusc.2004.05.091.

29. S. Anantathanasarn and H. Hasegawa, Photoluminescence and capacitance-voltage characterization of GaAs surface passivated by an ultrathin GaN interface control layer, *Applied Surface Science* **190** (2002) 343, https://doi.org/10.1016/S0169-4332(01)00840-6.

30. J. Osvald, R. Stoklas, and P. KordoÅ¡, Low- and high-frequency capacitance of aluminum gallium nitride/gallium nitride heterostructures with interface traps, *Materials Science in Semiconductor Processing* **31** (2015) 525, https://doi.org/10.1016/j.mssp.2014.11.052.

31. M. Amrani *et al.*, Study of lateral polysilicon PN diodes C-V characteristics: Modeling and experiments, *Solid-State Electronics* **42** (1998) 1925, https://doi.org/10.1016/S0038-1101(98)00180-4.

32. H. K. Gummel, A Self-Consistent Iterative Scheme for One-Dimensional Steady State Transistor Calculations, *IEEE Transactions on Electron Devices* **11** (1964) 455, https://doi.org/10.1109/T-ED.1964.15364.

33. D. R. Lide, CRC Handbook of Chemistry and Physics (2005), p. 3485, 978-1466571143.

34. N. Miura, et al., Thermal annealing effects on Ni/Au based Schottky contacts on n-GaN and AlGaN/GaN with insertion of high work function metal, *Solid-State Electronics* **48** (2004) 689, https://doi.org/10.1016/j.sse.2003.07.006.

35. M. Ogawa and T. Baba, Heavily si-doped gaas and alas/n-gaas superlattice grown by molecular beam epitaxy, *Japanese Journal of Applied Physics* **24** (1985) L572, https://doi.org/10.1143/JJAP.24.L572.

36. N. Watanabe, T. Nittono, and K. Watanabe, Annealing effect on the carrier concentration in heavily Si-doped n +-InGaAs, *Applied Physics Letters* **61** (1992) 1945, https://doi.org/10.1063/1.108371.